

RENATA DWORNICKA*

A COMPARATIVE ANALYSIS OF STRESS CONCENTRATION FACTOR CALCULATED FROM PN-EN 12952-3 CODE AND FROM FEM CALCULATIONS (ANSYS)

ANALIZA PORÓWNAWCZA WYZNACZANIA WSPÓŁCZYNNIKA KONCENTRACJI NAPRĘŻEŃ W OPARCIU O NORMĘ PN-EN 12952-3 I OBLICZENIA WYKONANE W PROGRAMIE ANSYS

Abstract

A non-homogeneous temperature distribution in an element and an affecting pressure are causes of stresses in the material of the element. Knowledge of these stress values is necessary for proper determination of stresses allowable for the element. One of the element stress components is thermal stress, caused by temperature difference Δt in the element wall. This article presents a comparison of stress concentration factor computations based on PN-EN 12952-3 code recommendations and computations based on FEM analysis conducted in ANSYS environment. The comparative analysis is performed for the drum-pipe joint of a drum boiler.

Keywords: thermal stresses, stress concentration factor, finite element method

Streszczenie

Chcąc poprawnie wyznaczyć naprężenia dopuszczalne w elemencie ciśnieniowym, konieczna jest znajomość wartości naprężeń składowych. Jedną ze składowych naprężeń w elemencie są naprężenia cieplne powstające na skutek różnic temperatur w ścianie. Artykuł przedstawia porównanie wyznaczenia wartości współczynnika koncentracji naprężeń pochodzących od temperatury, zgodnie z zaleceniami PN-EN 12952-3 i z obliczeniami wykonanymi w programie ANSYS. Analizę porównawczą przeprowadzono dla elementu, którym jest połączenie walczak – rura opadowa.

Słowa kluczowe: naprężenia cieplne, współczynnik koncentracji naprężeń, metoda elementów skończonych

* MSc. Renata Dwornicka, Institute of Applied Informatics, Faculty of Mechanical Engineering, Cracow University of Technology.

1. Introduction

A non-homogeneous temperature distribution in an element and an influential pressure are causes of stresses in the material of the element. Knowledge of these stress values is necessary for proper determination of stresses allowable for the element. Determination of thermal and pressure stresses depend mainly on a proper form of a stress concentration factor: in the case of pressure stresses $f_{\text{tang},p}$, it is the factor α_m whilst in the case of thermal stresses $f_{\text{tang},t}$, it is the factor α_t . PN-EN 12952-3 code introduced a rough method for calculation of stress concentration factor which may differ slightly from precise calculations. In this paper, the author compares results obtained from this code and from FEM analysis (ANSYS system) for a drum boiler.

2. Methodology of calculations based on PN-EN 12952-3

One of the element stress components is thermal stress $f_{\text{tang},p}$, caused by temperature difference Δt in the element wall. The stress is calculated by the following formula:

$$f_{\text{tan } g, t} = \alpha_t \cdot \frac{\beta_{L_t^*} \cdot E_{t^*}}{1 - \nu} \cdot \Delta t \text{ [MPa]} \quad (1)$$

where:

- $\beta_{L_t^*}$ – linear coefficient of thermal expansion,
- E_{t^*} – elastic modulus,
- ν – Poisson's ratio,
- Δt – temperature difference in the wall,
- α_t – stress concentration factor for thermal stresses.

Thermal stresses in the element depend on a proper form of stress concentration factor α_t appearing in the formula (1). Its value may be evaluated graphically from the plot (Fig. 1) published in [1] or numerically from the formula (2).

$$\alpha_t = \left\{ \left[2 - \frac{h+2700}{h+1700} \cdot z + \frac{h}{h+1700} \cdot (\exp(-7 \cdot z) - 1) \right]^2 + 0,81 \cdot z^2 \right\}^{\frac{1}{2}} \quad (2)$$

where:

- h – heat penetration factor,
- z – quotient of combined elements' diameters.

The quotient z is calculated from the formula (3):

$$z = \frac{d_{mh}}{d_{ms}} \quad (3)$$

where:

d_{ms} – average diameter of the body,

d_{mb} – average diameter of the pipe branch.

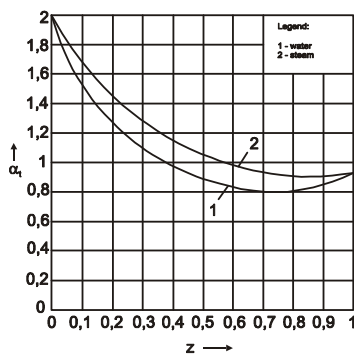


Fig. 1. Stress concentration factor α_t for thermal stresses in cylindrical and spherical shells

Rys. 1. Współczynnik koncentracji naprężeń wywołany naprężeniami termicznymi α_t dla powłok walcowych i kulistych

According to the codes, the heat penetration factor h is equal to 1000 W/m²K in the case of steam and is equal to 3000 W/m²K in the case of water.

3. FEM-based verification of results

Determination of the above-mentioned factor from the plot (Fig. 1), according to the recommendations of PN-EN 12952-3 code [1], is imprecise. For a higher accuracy of obtained results, the code recommends complex numerical methods e.g. the finite element method. A comparative analysis was conducted for an example element: the drum-pipe joint of a drum boiler (Fig. 2).

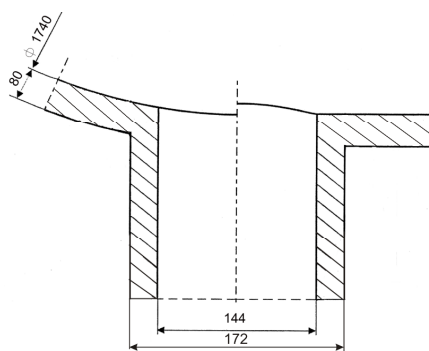


Fig. 2. Drum-pipe joint of a drum boiler

Rys. 2. Połączenie walczak – rura opadowa

As part of the analysis, stress concentration factors at were calculated from the formula (2) assuming a value of the heat penetration factor h equal to $3000 \text{ W/m}^2\text{K}$. Next, numerical calculations were conducted starting from an unweakened element (a pipe) modelled in ANSYS [2]. Owing to the symmetry of the element, modelling of a quarter was sufficient. The model was subsequently divided into solid elements (Fig. 3).

Calculations for a non-stationary thermal state were conducted with the following assumptions: starting temperature $t_0 = 20^\circ\text{C}$; heat penetration factor $h = 3000 \text{ W/m}^2\text{K}$; heating duration $T = 7000 \text{ s}$. The external surface of the element is thermally isolated while the internal surface is washed by a liquid. The convective boundary condition is defined for the whole internal surface. It is assumed that temperature varies from $t_0 = 20^\circ\text{C}$ at a constant rate $v = 3 \text{ K/min}$, whilst the liquid temperature distribution along the internal boundary is homogeneous. Additional assumptions were made for computations: temperature distribution was taken from thermal calculations and the element was settled so as to exclude any rigid movement [3].

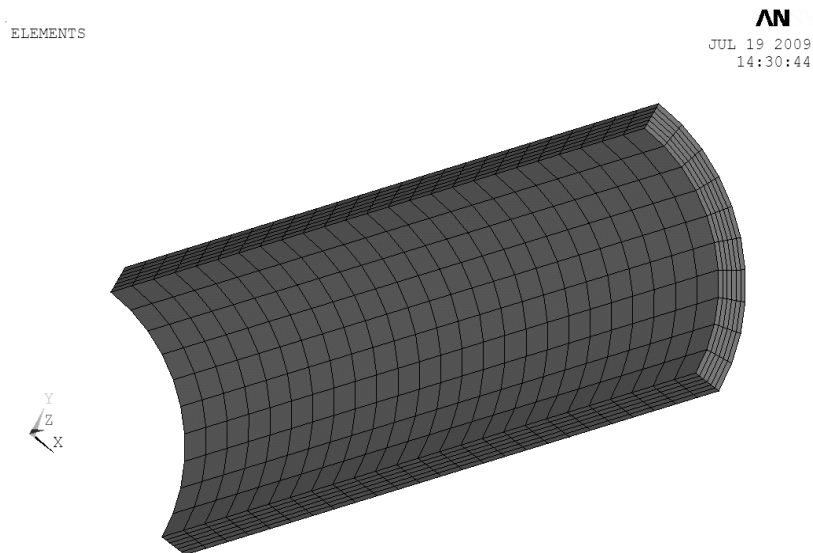


Fig. 3. FEM mesh applied to the unweakened element

Rys. 3. Nałożona siatka na elemencie nieosłabionym

4. Results

The minimum value obtained from FEM analysis conducted in ANSYS for circumferential stress in a quasi-stationary state system is equal to $f_{\text{tang},t} = -42,06 \text{ MPa}$ (Fig. 4). The distribution of the reduced thermal stresses in the unweakened element is presented in Fig. 5. The maximum value of the stress reduced according to the HMH hypothesis for the unweakened element is equal to $f_{\text{HMH},t} = 41,83 \text{ MPa}$.

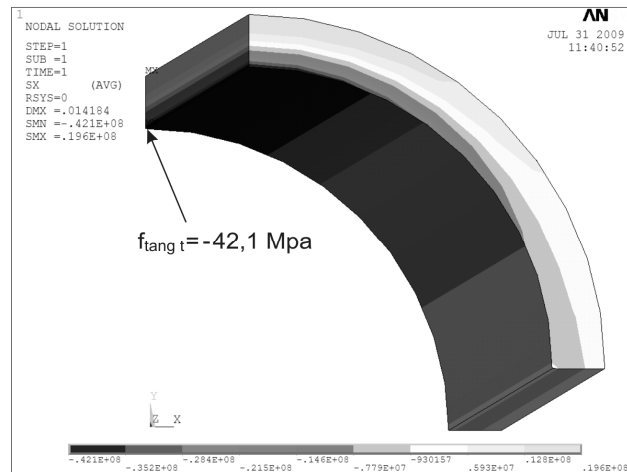


Fig. 4. Distribution of thermal stresses in the direction of the x-axis for the unweakened element

Rys. 4. Rozkład naprężeń cieplnych w kierunku osi x w elemencie nieosłabionym

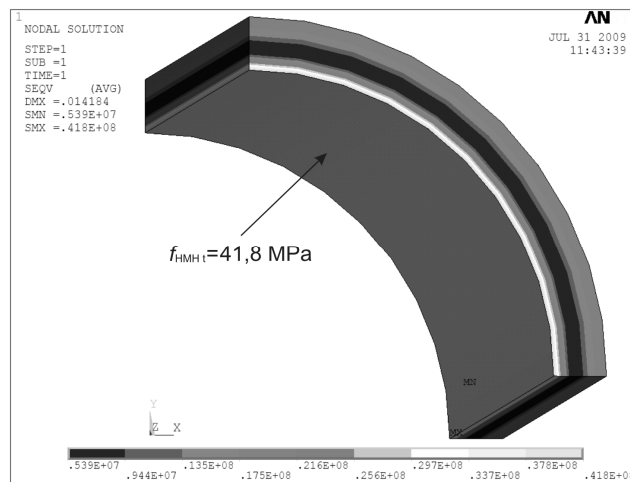


Fig. 5. Distribution of reduced thermal stresses for the unweakened element

Rys. 5. Rozkład zredukowanych naprężeń cieplnych w elemencie nieosłabionym

The weakened element was also modelled. As an example of computations of a quasi-stationary state, the joint presented in Fig. 6 was selected. Owing to the symmetry of the element, modelling of a quarter was sufficient. The obtained model was divided into solid elements. A finer finite element mesh was applied in those areas where the greatest stresses were expected. In the remaining areas, a coarse mesh may be imposed to shorten computation time.

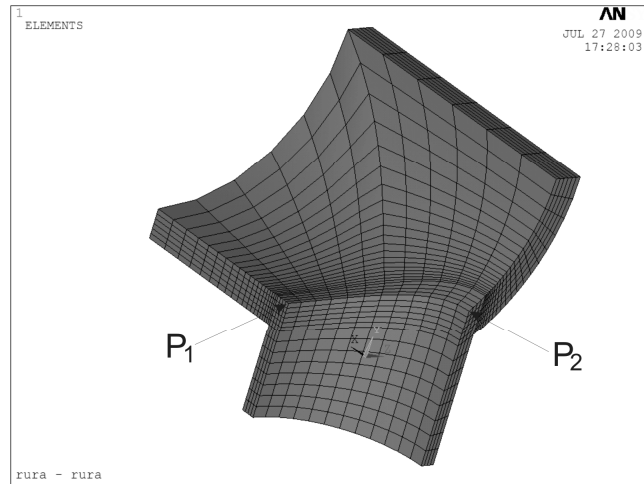


Fig. 6. FEM mesh applied to the weakened element

Rys. 6. Nałożona siatka na elemencie osłabionym

Control parameters and boundary conditions were similarly defined in the case of the unweakened element. After computations in ANSYS, a stress distribution for the weakened element was obtained. The circumferential stress at point P1 was calculated at $f_{\text{tang},t} P1 = -28,2$ MPa and at point P2 at $f_{\text{tang},t} P2 = -52$ MPa. The calculated stresses, presented in Fig. 7, are negative due to a compression related to surface heating. The circumferential stress at point P1 may be read as a stress in the direction of the z-axis, whilst the circumferential stress at point P2 may be read as a stress in the direction of the x-axis.

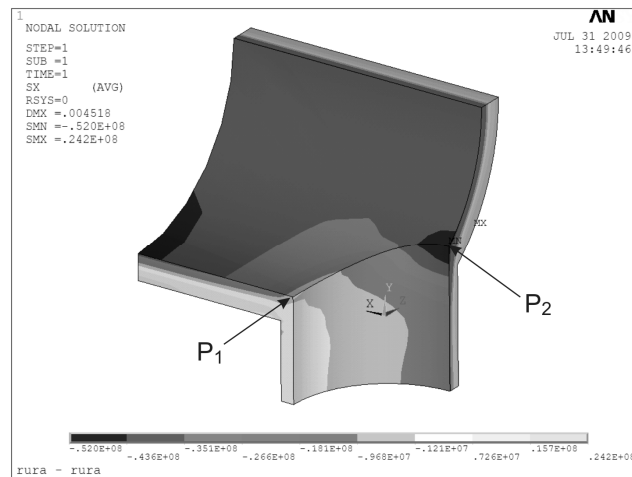


Fig. 7. Thermal stress distribution in the direction of the x-axis for the weakened element

Rys. 7. Rozkład naprężeń cieplnych w kierunku osi x w elemencie osłabionym

The distribution of reduced thermal stresses for the weakened element is presented in Fig. 8. The stress at P1 point is equal to $f_{\text{HMH},t P1} = 27,99$ MPa whilst at P2 point it is equal to $f_{\text{HMH},t P2} = 48,73$ MPa.

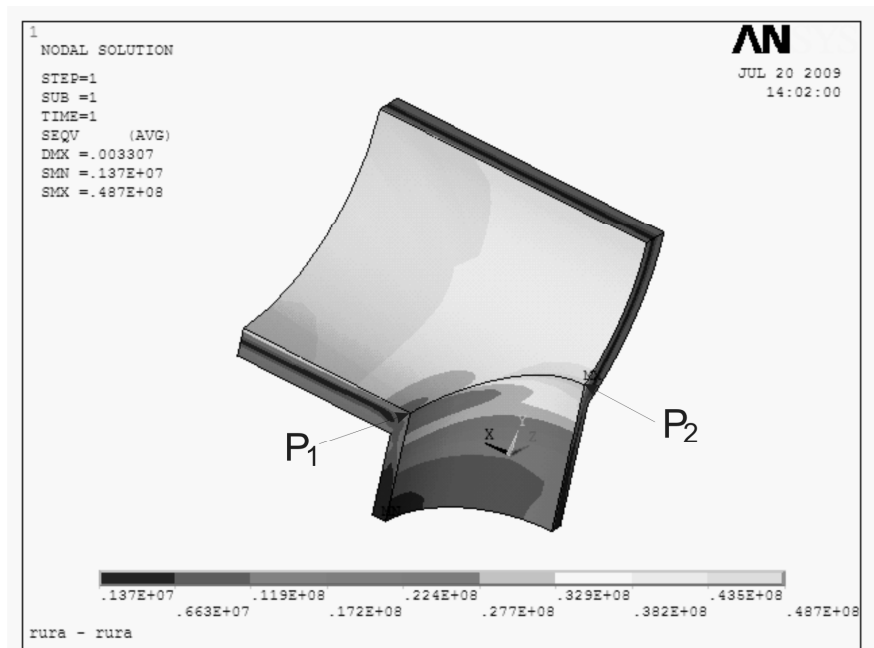


Fig. 8. Reduced thermal stress distribution for the weakened element

Rys. 8. Rozkład zredukowanych naprężeń cieplnych w elemencie osłabionym

5. Conclusions

The investigated elements were modelled in ANSYS. Minimum stress in the direction of the x-axis was determined for the unweakened element. Circumferential stresses at points P1 and P2 were also determined for weakened element. On the basis of their values, stress concentration factors α_t were calculated. It was assumed that α_t is a quotient of the maximum (according to absolute values) circumferential stress of the weakened element to the same stress of the unweakened element.

A comparison of stress concentration factors α_t obtained from the PN-EN code and from FEM analysis is presented in Fig. 9. The computations were repeated for different mesh densities and it was concluded that measurement sensitivity for different mesh densities is not significant. It is recommended to determine the stress concentration factor by FEM analysis as a more accurate method.

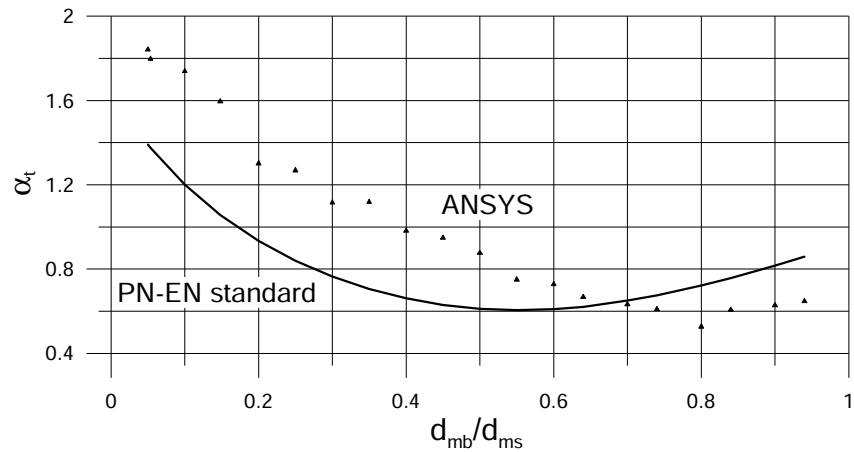


Fig. 9. A comparison of stress concentration factors α_t obtained from the PN-EN code and from FEM analysis

Rys. 9. Porównanie współczynników koncentracji naprężeń α_t otrzymanych w oparciu o normę PN-EN i w wyniku zastosowania metody elementów skończonych

References

- [1] PN-EN, Code 12952-3:2004/Ap1:2005.
- [2] ANSYS User's Manual, Revision 5.0 A.
- [3] Duda P., *Monitoring of the thermal and strength working conditions of power plant pressurized element, monograph*, Cracow University of Technology, Mechanic Course, Vol. 81, Kraków 2004.